

## Magnetic Characteristics of the DØ Detector

R. Yamada, D. Eartly, J. F. Ostiguy and H. Jostlein

*Fermi National Accelerator Laboratory  
P.O. Box 500, Batavia, Illinois 60510*

Y. Antipov, D. Denisov and S. Chekulaev

*Institute for High Energy Physics  
Protvino, USSR*

September 1991

\* Presented at the 12th International Conference on Magnet Technology, Leningrad, USSR, June 24-28, 1991.

# MAGNETIC CHARACTERISTICS OF THE D0 DETECTOR

R. Yamada, D. Eartly, J.F. Ostiguy, and H. Jostlein  
Fermi National Accelerator Laboratory  
Batavia, Illinois 60510, USA

Yu. Antipov, D. Denisov, and S. Chekulaev  
Institute for High Energy Physics, Protvino, USSR

## Abstract

In the D0 detector, muon momentum is measured by deflection through toroidal iron magnets. The general features of these magnets are discussed. We describe design calculations performed with the two-dimensional codes POISSON and ANSYS. Full three-dimensional calculations performed with the code TOSCA are also presented. Magnetic field and flux measurements are described and compared with the calculations.

## 1 Introduction

A perspective view of the Fermilab D0 hadron detector, located in the D0 straight section of the Tevatron collider and scheduled to be put in operation at the end of 1991 is shown in Figure 1. The detector has three distinct components: a central tracking detector, a liquid argon uranium calorimeter (3 cryostats), and a muon detector [1]. The latter consists of a set of toroidal magnets and a proportional drift chamber system [2, 3]. We concentrate here on the muon detector magnets.

The muon detector magnet system is composed of three principal toroids: the central toroid which we refer to as CF, and two end toroids which we refer to as EFs. The initial design of the D0 detector included a square aperture in the center of each EF toroid for a small end plug calorimeter. When the EF toroids were built, it was decided to eliminate the calorimeter and to fill the aperture with two small toroids, referred to as SAMUS (for Small Angle MUon Spectrometer).

The three major toroids are connected in series and powered by a Transrex power supply rated at 2500 A at 200 V. The power supply, based on a 12-phase SCR circuit, is connected in series with a 0.83 mH, 1.8 m $\Omega$  choke and a reversing switch. The two SAMUS toroids are connected in series and powered with a smaller PEI 150 kW power supply rated at 1250 A at 120 V. The total power consumption of the system is 0.5 MW. Although the power supplies generate a substantial amount of high frequency noise, we found no noticeable effect on the electronics located inside

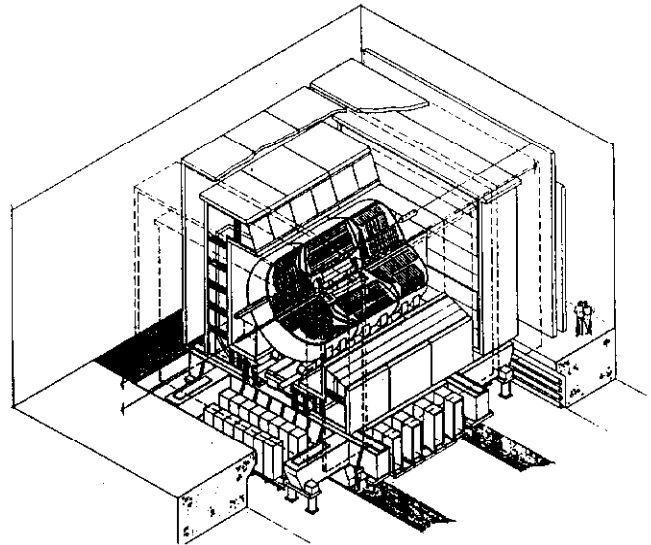


Figure 1: Perspective View of the D0 Detector.

and underneath the CF toroid.

The magnets are mounted on a platform, which moves the whole detector into the collision hall. The toroids account for about 70% of the total weight of the detector, which is approximately 5000 metric tons. For maintenance purposes, the central toroid is made of a fixed central base beam and two moving parts. Nonmagnetic stainless steel spacers inserted between the three pairs of mating surfaces reduce the remanent flux and facilitate separation of the moving parts. A selection of parameters is presented in Table 1.

## 2 Field Calculations

The flux distribution inside the toroids can, to a very good approximation, be regarded as two-dimensional; furthermore, because the flux is mostly confined inside the cores, one expects little interaction between the magnets. The CF, EF and SAMUS toroids were therefore designed separately using the two-dimensional codes POISSON and ANSYS. The code TOSCA was then used to obtain a detailed three-dimensional field map of the entire magnet system including the supporting platform. We intend to use this

Toroids	CF	EF(each)	SAMUS(each)
Axial dimension(cm)	757	152.4	167.6
Inner width(cm)	635	182.8	50.8
Outer width(cm)	852.2	833.2	170.2 (avg)
Weight(m.ton)	1973	800	32
Unit coils	20	8	2
Turns/coil	10	8	25
Current(A)	2500	2500	1000
Voltage(V)	107	19	46
Resistance(m $\Omega$ )	42.8	7.5	46
Average field (T)			
Top Yoke	1.90	1.84	1.99
Side Yoke	1.91	1.96	1.56

Table 1: Toroid Parameters.

three-dimensional field map in the detector tracking software.

## 2.1 BH Curves

The vertical yokes of CF were made from the retired SUREL cyclotron yoke originally built in the 1960's, using forged and cast iron. The top and bottom yokes of CF and all of EF's yokes were made of hot rolled distressed iron of 1010 quality. The SAMUS yokes were made of a mixture of Russian iron equivalent to 1008 and 1010 quality. The *BH* curve used for CF was adjusted to fit the flux measured in the top gap. For EF, we used manufacturer's data for 1010 non-annealed steel. Finally the *BH* curve used for the SAMUS toroids was obtained from sample data.

## 2.2 Design of CF

The central toroid CF on the supporting platform is shown in Figure 2. The central base beam which is fixed to the platform is made of three thick steel slabs, totaling 42-3/4 in high and 59 in wide, stacked and welded together. There are altogether 20 unit coils on the CF toroid, each consisting of 10 turns. Five unit coils are mounted on each vertical yoke, three unit coils on each top yoke and 2 unit coils on each bottom yoke.

There are three intentional gaps, 1/8<sup>th</sup> inch gaps on both sides of the central beam, and a 3/16<sup>th</sup> inch gap between the top mating surfaces of the west and east side yokes. These gaps facilitate the separation of the side yokes by reducing the remanent magnetic field when the power is turned off. Stainless steel plates are used as mechanical spacers. These plates do not entirely fill the gap and the magnetic field can be measured inside five slots.

The two-dimensional magnetic flux distribution for the right half of toroid is shown in Figure 3. The calculations were performed with the code POISSON [4]. The absence of coils in the central base beam region combined with the presence of two air gaps causes strong fringing fields. The flux leaking out around the central beam represents 3.7 % of the total flux circulating in the CF toroid.

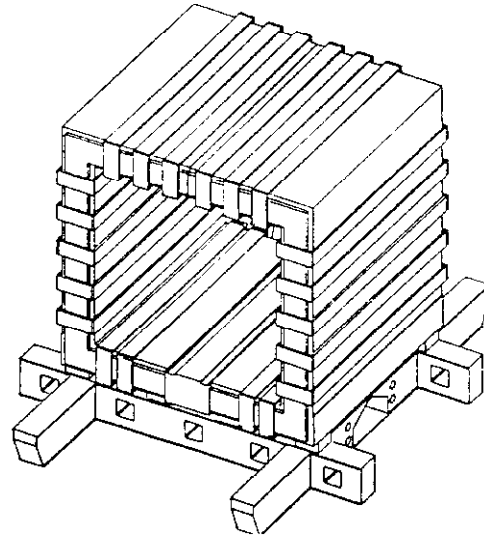


Figure 2: CF Toroid on Platform.

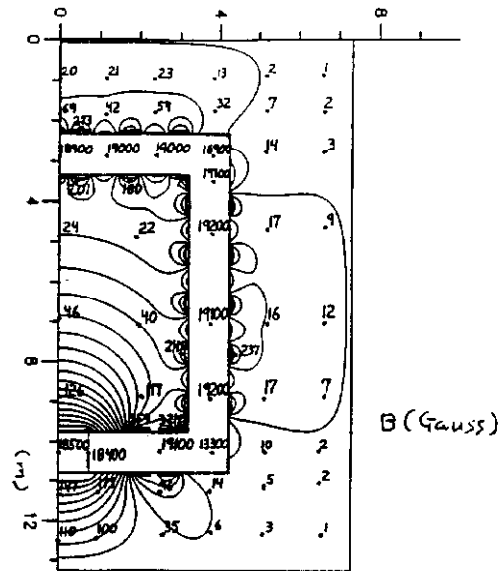


Figure 3: POISSON calculation for CF.

## 2.3 Design of EF and SAMUS

The EF and SAMUS toroids were first designed separately. Since the SAMUS toroids are inserted into the rectangular apertures of the EF toroids, calculations were also performed to understand mutual interference effects [5]. Two cases, corresponding to the two possible relative flux orientations, were studied. When the fluxes have opposite directions, the flux density is enhanced and more homogeneous in both toroids. When the magnetic fluxes in EF and SAMUS circulate in the same direction, the excitation currents in the interface region circulate in opposite directions. This results in inhomogeneous flux distributions in both toroids with a more pronounced effect in the SAMUS toroid as shown in Figure 4. Since muon tracking is considerably simpler when both fluxes are in the same direction, this alternative has been retained.

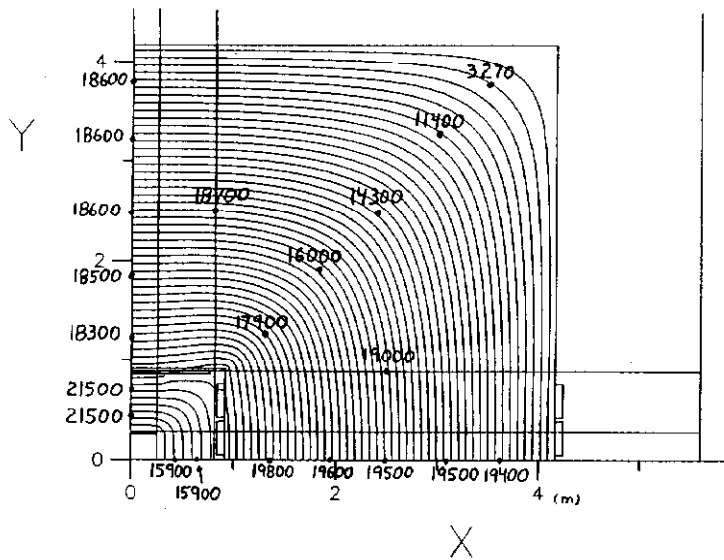


Figure 4: EF and SAMUS excited in the same direction with 2500 A and 1000A respectively.

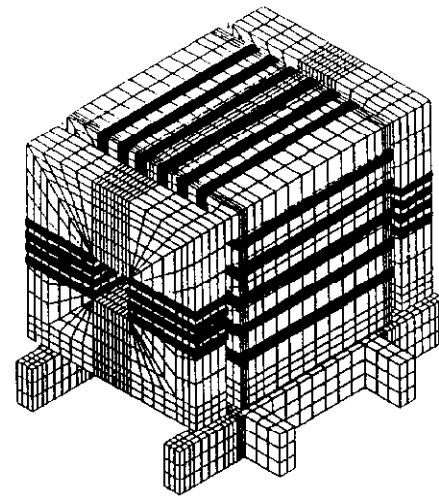


Figure 5: TOSCA model of the D0 Toroids.

## 2.4 Three-Dimensional Calculations

As mentioned earlier, the basic design of the muon detection system is based on strictly two-dimensional calculations. However, the following issues could not be addressed satisfactorily without recourse to full three-dimensional analysis:

- (1) The effect of the supporting steel platform on the flux distribution in the CF and EF.
- (2) The magnetic force between CF and EF.
- (3) The effect of the two EF toroids on the fringing field distribution inside the CF volume. This is important because the magnetic field may affect the performance of detector components mounted inside CF.
- (4) The effect of the finite axial extent of CF and EF on the flux distribution in the steel.

Calculations were performed on a Solbourne Series 5 model 800 workstation using the code TOSCA [6]. With 64 Mbytes of physical memory, the practical limit is of the order of 100,000 nodes, corresponding to a one-dimensional mesh resolution of approximately 46 nodes. Symmetry, judicious positioning of the nodes and quadratic interpolation have been used to maximize accuracy. An isometric view of the mesh showing quadratic element boundaries is shown in Figure 5.

The calculations show that the presence of the platform, made of 6 cm thick steel plates, results in a 1.3 % decrease of the flux in the CF toroid bottom yoke. There is a 4.5 kN attractive magnetic force between the CF and each EF toroid which is of no practical consequence. Finally, compared with the results obtained from two-dimensional analysis, the agreement between the measured and calculated fringing field distribution is noticeably improved [6].

## 3 Measurements

The magnetic field distribution in the CF gaps and the fringing field were measured using Hall probes. The magnetic flux was measured using flux loops wound on the yokes of toroids.

### 3.1 Field Measurements

The magnetic field distributions inside the three CF gaps were measured using a Hall probe for  $I = 2190$  A. The field distribution in the central beam gaps was measured at several positions and the average of the field distribution is plotted in Figure 6. The variation of the field in the vicinity of the top surface is due to a variation in the gap width. The two dips in the field distribution are caused by concave weldment edges of the three 14-inch thick steel plates which form the central base beam. The average field value in the center beam gap is 1.789 T at 2190 A.

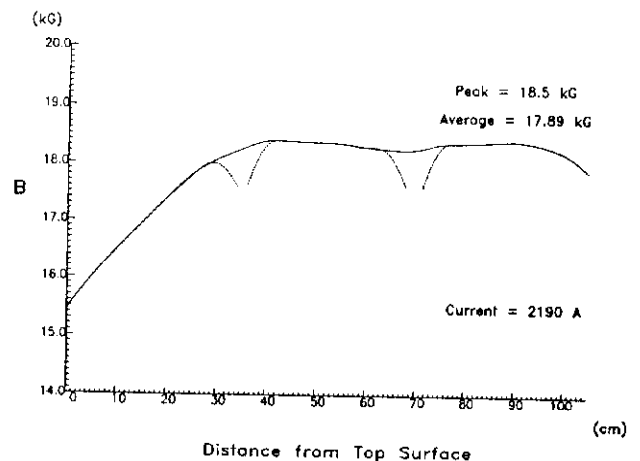


Figure 6: Average  $B$  in the Center Beam gap at 2190 A.

The field was also measured in the top gap at several locations along the longitudinal dimension for  $I = 2190$  A.

The field increases from 1.776 Tesla at the edge of the gap to a maximum of 1.902 Tesla at the center. The average value of the field in the top gap is 1.866 T. The gap is nominally  $3/16$  inch at both edges where  $3/16$  inch stainless steel plates are welded. However, the mating surfaces of the top gap have not been machined completely flat and the gap is about 7% (0.3mm) smaller at the center of the yoke.

The field at 2500 A can be obtained by extrapolating the measurements at 2190 A. Taking the excitation curve into account, the field is estimated at 1.89 T in the top gap and 1.82 T in the bottom gap. The 4.2 % difference between these two values is in good agreement with the prediction of the two-dimensional calculations.

### 3.2 Flux Measurements

Flux loops were used to measure the flux distribution in each of the three toroids. To obtain spatial resolution, loops were positioned through the body of the toroids. The toroids were fabricated by welding thick steel plates and thin slots were purposely left whenever possible to allow passage of the flux loop conductors.

Six loops were wound across the vertical yoke of the CF toroid. Twelve loops were wound on each of the EF toroids and eighteen loops were wound around the SAMUS toroid.

For data acquisition and analysis we used a 40-channel Macintosh based system with a combination of a high accuracy scanner and a 6-1/2 digit digital multimeter [7]. With each loop assigned to a different channel, the induced electromotive force was sampled and numerically integrated. A full measurement cycle (40 channels) took 8.3 seconds; the measurement speed was limited by software considerations. The toroid excitation current was cycled a few times between  $\pm 2500$  A over a period of two hours. To minimize errors introduced by the low sampling rate, an  $RC$  low-pass filter ( $\tau = 15$  s) was connected at the input of each channel.

The signal induced in a loop was of the order of 10 to 40 mV and included a 0.18 mV thermoelectric voltage. Figure 7 shows the integrated signal for one of the loops mounted on the CF toroid. The thermoelectric drift has been subtracted out. The middle horizontal line corresponds to the true zero flux. The measured flux is the average of the magnitude of the peak flux values.

There were three runs for the flux measurement. In the first run, the CF and two EF toroids were excited together without SAMUS toroids [7]. The measured flux densities at 2500 A inside CF and EF were respectively 1.84 and 1.93 T in the vertical yokes. The remanent flux circulating in CF at zero current was 1.7 kG. Due to the absence of air gaps, the remanent flux in EF varied from 1 to 4 kG depending on previous history. In the second run only the two SAMUS toroids were excited [8]. In the third run, the North EF and corresponding SAMUS toroids were excited simultaneously with their nominal maximum currents [9]. The measured flux densities in EF and SAMUS are listed in Table 1.

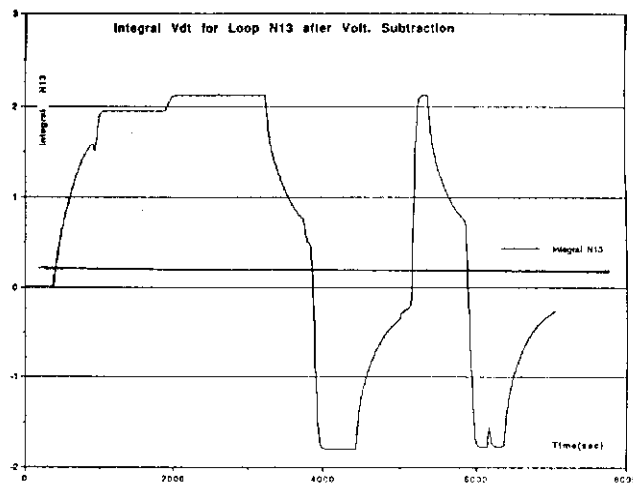


Figure 7: Integrated output of a typical flux loop.

## 4 Acknowledgments

The authors would like to acknowledge the contribution of the members of the D0 collaboration.

## References

- [1] "The D0 Experiment at the Fermilab Antiproton-Proton Collider", Design Report, Fermilab (1984).
- [2] C. Brown et al., "D0 Muon System with Proportional Drift Chambers", *Nucl. Instr. and Meth.*, A279, 331 (1989).
- [3] R. Yamada, "The Magnetic Design and Field Measurement of Fermilab Collider Detectors: CDF and D0", *Proceedings of 11th Int. Magnet Tech. Conf.* p.308 (1989).
- [4] R. Yamada and P. Lee, "Magnetic Field Calculation of CF Toroid", Fermilab D0 Note No. 833, (1989).
- [5] K. Hodel and R. Yamada, "Magnetic Field Calculation of SAMUS and EF Toroids", Fermilab D0 Note No. 1000, (1990).
- [6] J-F. Ostiguy and R. Yamada, "Three-Dimensional Field Map of the Fermilab D0 Detector", To be published in: *Proceedings of 1991 National Accelerator Conf. San Francisco, USA*.
- [7] H. Jostlein, "D0 Toroid Field Measurements from April 19, 1989", Fermilab D0 Note No. 846, (1989).
- [8] H. Jostlein and S. Chekulaev, "June 1990 Field Measurements on SAMUS Toroids on the Sidewalk", Fermilab D0 Note 1036 (1990).
- [9] H. Jostlein, "D0 EF/Samus Toroid Field Measurements of December 15 1990", To be reported in a forthcoming D0 Note.